Effects of Waxes and the Related Chemicals on Asphaltene Aggregation and Deposition Phenomena

Article

Effects of Waxes and the Related Chemicals on Asphaltene Aggregation and Deposition Phenomena: Experimental and Modeling Studies

Edris Joonaki,* Aliakbar Hassanpouryouzband, Rod Burgass, Alfred Hase, and Bahman Tohidi

Read Online

| ACCESS | Metrics & More | Article Recommendations | SI Supporting Information |

ABSTRACT: Solid deposition during production, transport, and storage of crude oils leads to significant technical problems and economic losses for the oil and gas industry. The thermodynamic equilibrium between high-molecular-weight components of crude oil, such as asphaltenes, resins, and waxes, is an important parameter for the stability of crude oil. Once the equilibrium is disturbed due to variations in temperature, pressure, and oil composition during production, the solubility of high-molecular-weight waxes decreases. This results in a decrease in the wax appearance temperature (WAT) and the deposit of wax onto solid surfaces. On the other hand, under these conditions, asphaltenes do not interact sufficiently with the resins/waxes and tend to flocculate among themselves and form asphaltene nanoaggregates. The role of waxes during the asphaltene aggregation and deposition has not been appropriately explained yet. The objective of this research study is to describe the interaction of asphaltenes and waxes and subsequently address the specific example of an asphaltenic oil commingled with a wax inhibitor-containing oil during the combination of different oil streams. It is a crucial building block for the development of a suitable and cost-effective strategy for the handling of wax/asphaltene associated flow assurance problems. In this work, the quartz crystal microbalance (QCM) technique has been used for the first time to investigate the effect of waxes and related chemicals, which are used to mitigate wax deposition, on asphaltene aggregation and deposition phenomena. Asphaltene onset point and asphaltene deposition rate have been monitored using QCM at high pressure–high temperature (HPHT) conditions. This study confirms that the different wax inhibitor chemistries result in significant differences in the pour point decrease and viscosity profiles in crude oil. Different wax inhibitors also showed different outcomes regarding the asphaltene deposition tendency. A comprehensive modeling study has also been conducted for mechanistic investigation of experimental results. In this regard, the perturbed chain statistical associating fluid theory equation of state (PC-SAFT EoS) was utilized to model the systems.
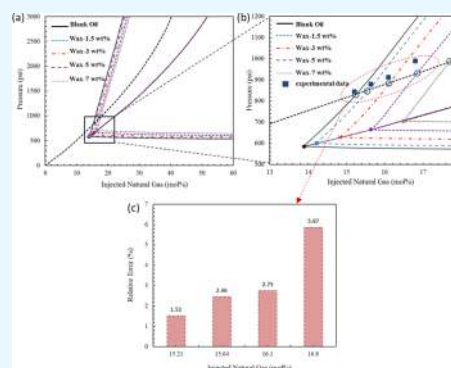
1. INTRODUCTION

Organic solid deposition is a serious challenge in the oil industry, from production to oil transportation and storage operations.[1] Paraffin wax can affect the rheological properties and asphaltene phase behavior in the oleic phase by using wax components used in the asphalt industry (asphalt binder) and by blending different crude oils or oil with light or heavy paraffinic compounds.[2,3] From a chemical composition viewpoint, although the high-molecular-weight normal paraffins are the major moieties in wax deposits, long iso- and cycloalkanes and high-molecular-weight polyaromates named asphaltenes also exist.[4] On the other hand, the asphaltenes extracted from oil tank deposits contain a large amount of waxes.[5]

Asphaltenes are heavy and highly polar molecules found in crude oil, which contain polycondensed aromatic sheets and aliphatic chains along with various polar functional groups such as pyridine, pyrrole, hydroxyl, sulfoxide, carboxyl, and carbonyl.[6–10] Asphaltene aggregation and deposition may lead to wettability change in the rock surfaces toward oil-wet,

the formation of water in oil emulsion, formation damage, and plugging of the pipelines.[11–16] Asphaltenes precipitate and aggregate in crude oils as a result of alterations in the pressure and temperature or composition, such as a normal alkane when mixed with crude oil.[17] Generally, asphaltenes are described as the fraction of crude oil that is soluble in aromatic compounds (e.g., toluene or xylene) but insoluble in low-molecular-weight n-paraffins (e.g., n-pentane, n-hexane, or n-heptane).[18–21] Paraffin wax is one of the main components of crude oil, well-known for being straight, ring form, and/or branched alkanes with high carbon atom numbers, e.g., more than 18.[22,23] Wax can cause serious challenges such as adhering to
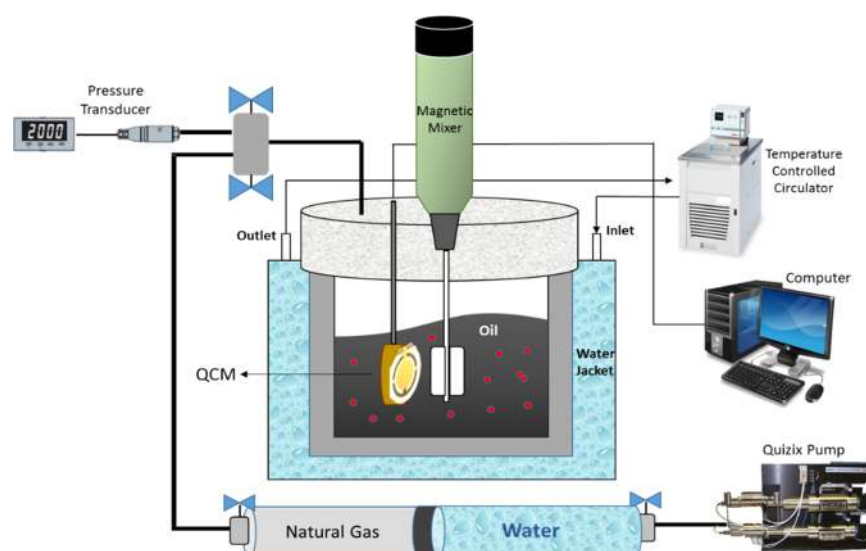
Figure 1. Schematic diagram of the HPHT-QCM setup.

the pipeline surfaces and restricting flow. Additionally, it can lead to increased viscosity, decreased flow, and an increase in operational costs. The major concern is the formation/appearance of wax at the highest temperature, at which the crystallization of wax can occur, known as the wax appearance temperature (WAT).[24] There are different experimental techniques that are utilized to determine the WAT, such as light scattering (near-infrared (NIR) and ultraviolet (UV) spectroscopy), cross-polarization microscopy (CPM), differential scanning calorimetry (DSC), viscosity measurement using a rheometer, and a quartz crystal microbalance (QCM).[25−28] Pour point is defined by ASTM D97 as the lowest temperature, considerably lower than WAT, at which a liquid loses its flow characteristics due to an increase in the amount of precipitated wax.[29] Various chemicals can be employed as wax inhibitors, such as ethylene vinyl acetate copolymers, vinyl acetate olefin copolymers, polyalkylacrylates, alkyl phenols, and α olefin copolymers, to address related flow assurance issues through pour point depression and/or wax precipitate despersancy.[30,31]

The role of asphaltenes during wax crystallization has not yet been well understood. The influence of asphaltenes has been explained contradictorily. Some researchers noted no significant interactions between wax and asphaltenes, but that asphaltenes may result in smaller interspersed wax crystals.[32,33] Others have claimed that asphaltenes worsen the paraffin wax associated flow assurance problems.[4,34] On the other hand, asphaltene solubility in various light n-paraffin solvents has been studied using optical microscopy,[35] light scattering,[36] refractive index,[37] and UV−vis spectrophotometry[38] and has been widely reported in the literature. Some asphaltene properties, such as molecular mass distribution, density, and solubility parameters, are fitted and adjusted using the aforementioned experimental data of asphaltene precipitation yield curves.[39,40] Fitted curves can be utilized to determine the asphaltene phase behavior in other chemical compositions (changing precipitant agents) or different pressure and temperature conditions.[41,42] On the other hand, some studies are reported in the literature for the role of light n-alkane precipitants on the precipitation behavior of asphaltenes.[43−45] At high n-alkane contents, the yield of asphaltene precipitates

was shown to increase with reduced n-alkane chain length.[43] This behavior demonstrates that n-alkanes with shorter chains are more potent asphaltene precipitants compared to those with longer chains. This observation is consistent with solubility parameters observed for smaller short-chain alkanes. Furthermore, some experimental results depict that the minimum amount of a precipitant (onset vol %) required for asphaltene destabilization passes through a maximum due to the increase in the carbon number of the precipitant.[44] The n-alkane chain length at the maximum varies among carbon numbers ranging from 7 to 10 according to the literature.[43,44] The entity of a maximum in the onset volume as an increase of the carbon number denotes that the precipitating strength of n-alkanes does not alter uniformly with alterations in the precipitant's chain length. This suggests that the precipitating potency of the n-alkanes decreases with an increase in the carbon number up to a maximum value and then increases beyond this value. This observation is mainly due to the entropy of the mixing of molecules with various sizes. The Flor−Huggins theory is widely employed to illustrate the phase behavior of asphaltenes.[46−49] Some researchers have highlighted the presence of the maximum carbon number at the onset point using various approximations to the regular Flory−Huggins theory.[44,50] Haji-Akbari et al.[43] investigated the aggregation kinetics of destabilized asphaltenes as a function of the carbon number of n-alkane precipitants. Despite a uniform change in the viscosity and solubility parameter, the asphaltene aggregation rate did not differ uniformly with the carbon number of n-alkane. Their model also successfully estimates the asphaltene aggregation rates in the presence of various n-alkanes and depicts that the most unstable fraction of asphaltenes with the highest solubility parameter is able to precipitate in the presence of greater n-alkanes.

Although the effect of different light n-paraffin solvents on the asphaltene phase behavior has been extensively investigated, the potential effects of heavy paraffins and their related chemicals on both asphaltene precipitation and deposition phenomena in the presence of gas have not yet been unveiled. The aim of this study is to shed some light on the effect of waxes and related chemicals on asphaltene solubility and stability in crude oil. First, the performance of various wax
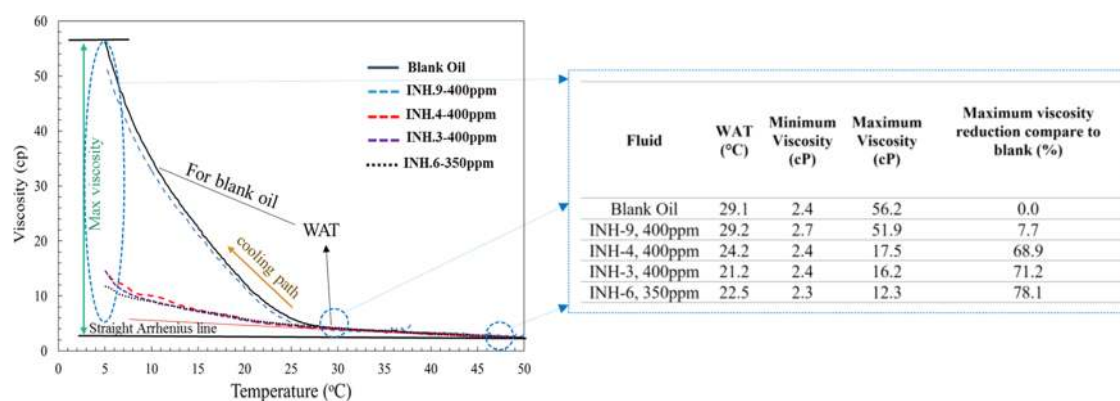
Figure 2. Results of rheometer tests with atmospheric geometry and shear rate of 10 s^{-1} using blank crude oil and blended with various wax inhibitors. The viscosity changes have been observed due to decrease in temperature for the blank crude oil and in the presence of various inhibitors at specified concentrations.

inhibitors in pour point decrease and WAT changes was evaluated by viscosity measurements using a rheometer. Then, a long-chain paraffin, as the main constituent of paraffinic crudes, and wax inhibitors at various concentrations were separately blended with crude oil, and their effects on the precipitation and deposition of asphaltenes of the treated oils were studied using a QCM-based technique. A modeling investigation was also conducted for the mechanistic understanding of observations from the experiments. The precipitation of asphaltenes from intact crude oil and paraffin wax-modified oils was thermodynamically modeled using perturbed chain statistical associating the fluid theory (PC-SAFT) equation of state; a good agreement between experimental and modeling results was achieved (Figure 1).

2. RESULTS AND DISCUSSION

2.1. Performance of Different Wax Inhibitors: WAT and Pour Point Determination.
Four commercial wax inhibitors have been employed to investigate their effect on WAT, pour point, asphaltene precipitation, and deposition phenomena using two different techniques, "rheometer" and 'high pressure−high temperature (HPHT)-QCM", which have been described in the Introduction. The efficiency of each additive was evaluated based on the decrease in the non-Newtonian viscosity when it was added to the system. In all cases, the viscosity obtained at the lowest temperature is the "maximum viscosity", which was intended to be used to evaluate the inhibitor performance. Figure 2 illustrates the viscosity changes (cP) with decrease in the temperature (°C) for the blank crude oil and for crude oil with various inhibitors at supplier-specified optimum concentrations.

As the cooling process started well above the wax appearance temperature, the viscosity gradually increased. This behavior continued following the Arrhenius temperature dependence of Newtonian fluids until the wax started to precipitate out from the crude oil. Equation 1 explains a linear Arrhenius relationship for the Newtonian range[51]

$$\mu = Ae^{-E_a/RT} \tag{1}$$

where μ is the Newtonian dynamic viscosity, E_a is activation energy of viscous flow in joules, R is universal gas constant, T is the temperature, and A is the pre-exponential factor largely dependent on the entropy of activation of flow. A sudden deviation in the viscosity was then observed owing to the formation of wax crystals. The point at which a non-Arrhenius

behavior began is considered as the WAT. As the temperature decreased further below the WAT, wax crystals grew causing the oil sample to become more non-Newtonian, and therefore the viscosity increased at a higher rate. The viscosity variations in the mixtures of oil + wax inhibitors were noticeable. It was also observed that the viscosity in the non-Newtonian region decreased in the presence of all inhibitors, particularly the polymeric ones.

Typically, the performance of wax inhibitors can be categorized in one of three classes: (1) decrease in high viscosity, (2) moderate decrease, and (3) no significant change or slight increase. As can be seen from Figure 2, inhibitors INH-3, 4, and 6 are placed in Class 1, and INH-9 is placed in Class 3. As an overall ranking, INH-3 and 6 were found to be better viscosity modifiers compared to the other tested inhibitors. The efficiency of wax inhibitors can also be evaluated based on their capability to reduce the pour point. The decrease in pour point may lead to higher production rates and therefore lower production costs for the operators.

The angular frequency, frequency, and amplitude torque for all of the pour point measurements were 10 rad/s, 1.6 Hz, and 25 μN m, respectively. The experimental conditions and results of the pour point variations owing to the presence of different wax inhibitors at their optimum concentrations using the rheometer in oscillation mode are depicted in Figure 3.

The liquid-like behavior of the reservoir fluid is identified by the loss modulus (viscous response), while the solid-like behavior is identified by the storage modulus (elastic response). When the wax−oil mixture was at a temperature above the pour point, the loss modulus was at a higher value than the storage modulus. When temperature decreased, both moduli values increased until the test fluid reached the pour point. At the pour point, the storage modulus is equal to the loss modulus. The storage modulus increased if the mixture was subjected to further cooling. Figure 3 clearly shows the role of wax inhibitors in the decrease of in the pour point for the treated oil sample.

All of the chemicals decreased the pour point with almost keeping a similar efficiency as they had for decrease of viscosity. INH-4 and 6 could decrease the pour point as better depressants from −5.29 to −25 °C and −23.6 °C, respectively.

2.2. Effect of Wax and Related Inhibitors on Asphaltene Instability.
The asphaltene aggregation and deposition experiments were conducted at and above the natural gas contents of the precipitation onset point. A HPHT-
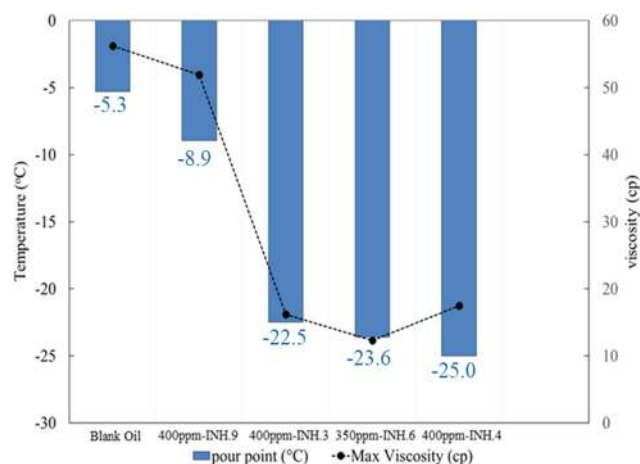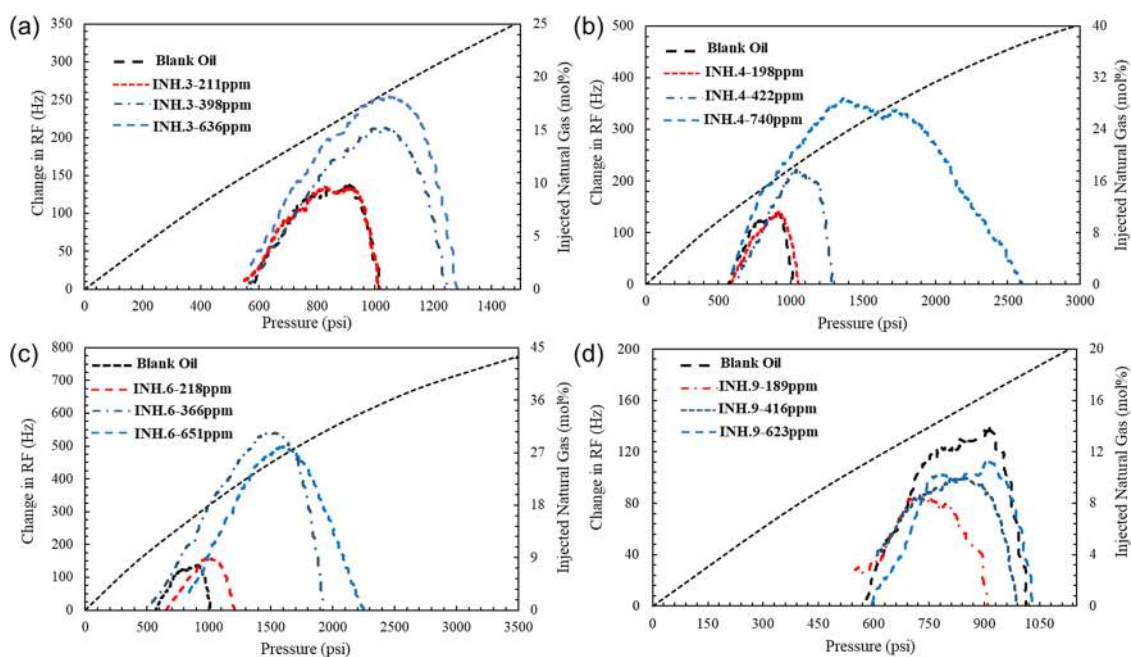
Figure 3. Results of the effect of wax inhibitors on decrease of the pour point for the blank crude oil and the modified ones with different wax inhibitors using the rheometer on the oscillation mode with an angular frequency of 10 rad/s, frequency of 1.6 Hz, amplitude torque of 25 μN m, and the destination temperature in the range of −20 to −25 °C.

QCM has been utilized in this study to investigate the effectiveness of paraffin wax and different wax inhibitors on the asphaltene precipitation and deposition rate at elevated pressure and temperature conditions in the presence of natural gas. The change in resonance frequency (RF) was monitored during the natural gas injection to determine the asphaltene precipitation onset point and the respective injected natural gas/oil ratio (GOR (mol %)), which is mixed with crude oil within the QCM cell. Herein, the asphaltene onset point of precipitation (AOP) is defined as the lowest natural gas/oil ratio at which asphaltene precipitation/inclination in the change in RF of QCM is first observed after a stepwise pressure increase process. The obtained results for AOP

determination and the effects of various wax inhibitors on asphaltene aggregation and deposition rate onto the QCM surface are given in Figure 4a−d. The change in RF increases as a result of a decrease in both viscosity and density of the fluid due to gas injection and decreases when asphaltenes start precipitating out of the crude oil. The pressure at which the RF starts to decrease represents the AOP, that is, ∼844 psi at ∼15.21 mol % of the injected gas for blank crude oil without any wax inhibitor. The AOP/GOR is ∼1561 psia/26.11 mol % for INH-6, ∼1082 psia/19.35 mol % for INH-4, ∼ 1047 psia/18.71 mol % for INH-3, and ∼847 psia/15.11 mol % for INH-9 with concentrations of 366, 422, 398, and 416 ppm, respectively, all close to the optimum concentrations that have been used for WAT and pour point depression tests.

Figure 5 shows the AOP and GOR obtained by HPHT-QCM versus different concentrations of wax inhibitors. The black square dot line curve in Figure 5 is the respective injected natural gas/oil ratio (mol %) for each AOP. Therefore, the representative AOP and GOR for each inhibitor at a given dosage rate can be identified. As can be observed, INH-6 performs well in comparison with three other wax inhibitors on changing AOP and the respective GOR (mol %). INH-9 is actually neutral with respect to changing asphaltene precipitation tendency at concentrations of 189 and 416 ppm and has shown some limited effects in suppressing asphaltene precipitation at 623 ppm.

The effect of each wax inhibitor with different concentrations on the comparative deposition rate, which is decrease in RF versus time, after the AOP is presented in Figure 6a−d. The results obtained clearly show that all employed wax inhibitors, with the exception of INH-9, have a positive effect on the asphaltene rate decrease on the QCM surface after exceeding the AOP. As can be seen, INH-9 at concentrations of 189 and 416 ppm increases the deposition rate from −316.4 to −369.1 and −327.8 Hz/h, respectively.

Figure 4. Results of the HPHT-QCM experiments for the examined crude oil with wax inhibitors: (a) INH-3, (b) INH-4, (c) INH-6, and (d) INH-9 at different concentrations. Black square dot line is the respective injected natural gas mole percentage (gas/oil ratio, GOR), which is mixed with crude oil within the QCM cell.
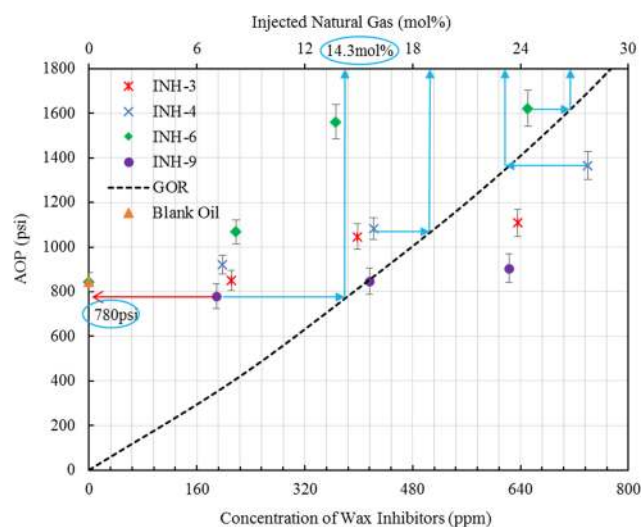
Figure 5. AOP/GOR versus concentration of four wax inhibitors: INH-3, 4, 6, and 9.

In addition, there is a drastic change in deposition rate curves between the blank oil and with 366, 398, and 422 ppm of inhibitors INH-6, 3, and 4, respectively. INH-6 has much better performance in decreasing the asphaltene deposition rate from −316.4.3 to −55.3 Hz/h compared to wax inhibitors INH-3 and 4 at the optimum concentration, which decreases the deposition rate to −192.1 and −219.6 Hz/h, respectively. A dramatic change in RF can be seen during the first 2 h of the experiment without an inhibitor, compared to the test with wax inhibitors. The ranking of wax inhibitors based on changes in AOP/GOR alterations and decrease in deposition rates obtained using the HPHT-QCM method is as follows: INH-6 > INH-4 > INH-3 > INH-9. As described in Table 2, INH-3 contains naphthalene and 1,2,4-trimethylbenzene, which can

interact with asphaltene nanoaggregates through a π-stacking interaction with aromatic cores of asphaltenes. However, it cannot properly curb further interaction between nano-aggregates since it does not have any strong surface-active functional group to interact with asphaltene molecules through hydrogen bonding, acid−base, or van der Waals interactions.[52−55] On the other hand, INH-6 has polymeric structures in aromatic solvents, and in addition to $\pi−\pi$ interactions, they could also create steric repulsion between the aliphatic tails of polymers and the asphaltene nanoaggregates. The enhanced performance of INH-6 in this study may be due to the influence of this steric repulsion on AOP and the resultant decrease in deposition rates. On the other hand, it is worth noting that generally INH-3, 4, and 6 in the presence of an aromatic solvent show superior performance in decreasing asphaltene precipitation and deposition. This is due to the ability of the solvent to control the phase behavior of the asphaltenes, which is dominated by dispersion forces.

The effect of wax at different dosages on asphaltene precipitation and deposition was also tested using HPHT-QCM. The AOP- and QCM-based deposition rates were considered as representative performance criteria for the ability of waxes to act as an inhibitor or promoter. Figure 7a shows an increase in AOP/GOR with the addition of paraffin wax. Hence, the addition of whole waxes appears to improve the solubility of asphaltene nanoaggregates in crude oil and the stability of asphaltenes increases with the increasing wax concentrations used in this study.

Figure 7b indicates that the addition of whole waxes could decrease the asphaltene deposition rate on the QCM surface for all samples tested. As can be observed, 5 wt % addition of wax to the crude oil can result in the decrease of the deposition rate from −316.4 to −60.3 Hz/h. Asphaltene precipitation is therefore affected by an ensemble of waxes with long aliphatic chains. It is proposed that waxes with various aliphatic chains
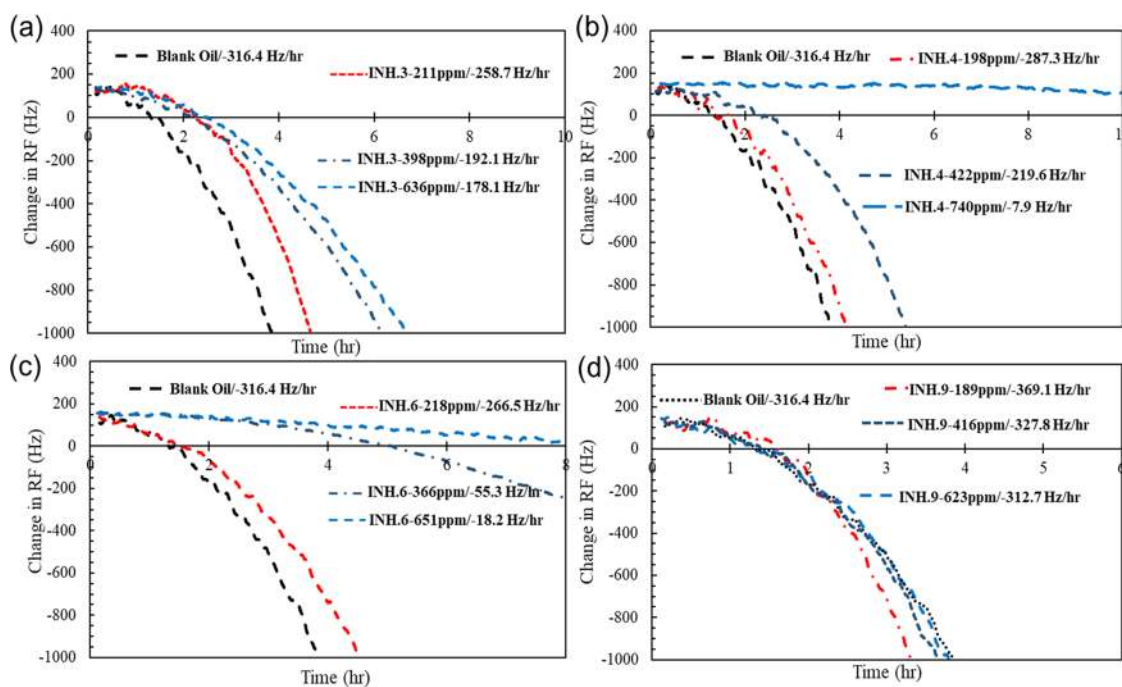
Figure 6. Results of the effect of different wax inhibitors: (a) INH-3, (b) INH-4, (c) INH-6, and (d) INH-9 on the asphaltene deposition rate at various concentrations.
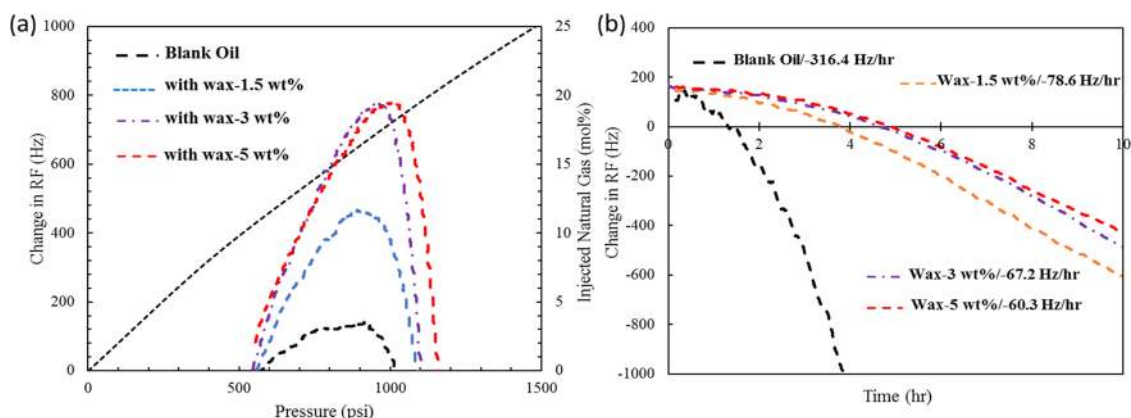
Figure 7. Effect of addition of various concentrations of wax to the crude oil on (a) AOP/GOR and (b) representative asphaltene deposition rate.
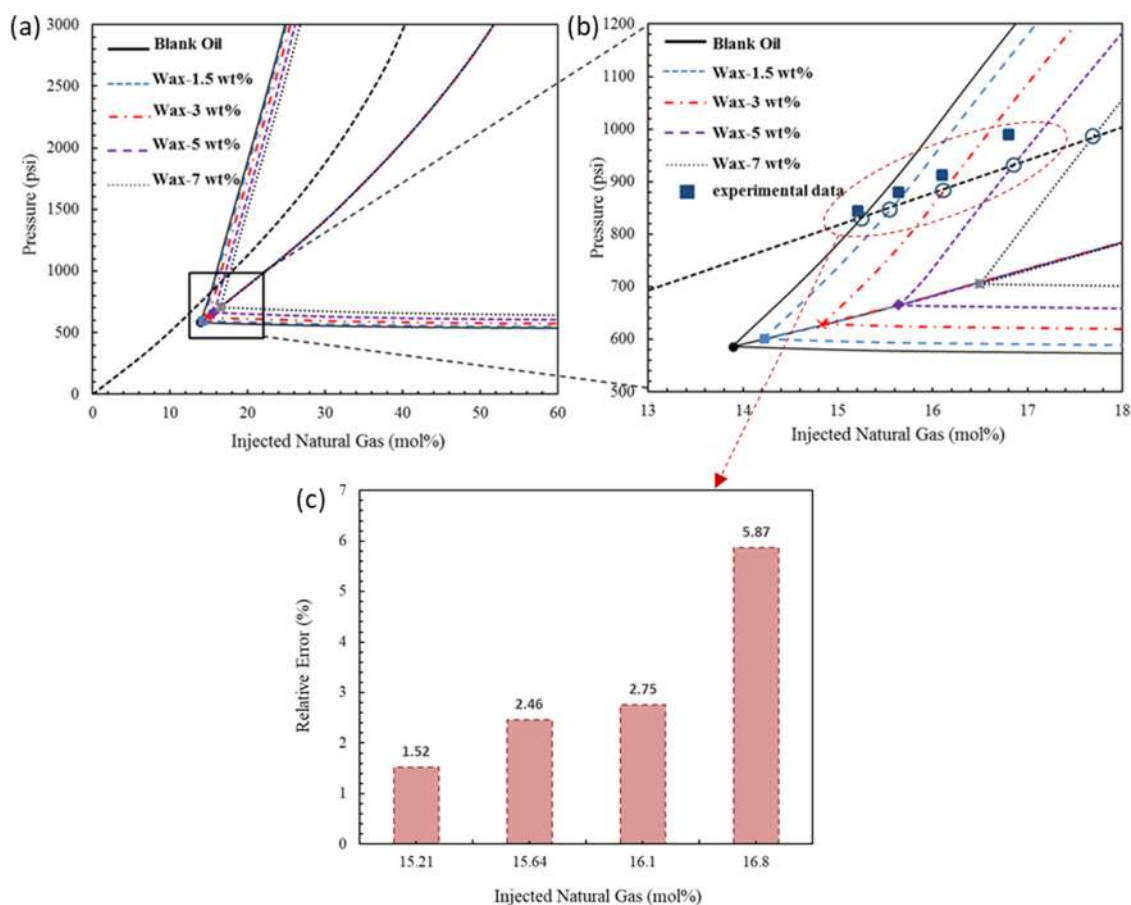
Figure 8. PC-SAFT modeling results of the effect of wax addition to the crude oil on asphaltene stability at various concentrations of 1.5, 3, 5, and 7 wt %: (a) modeling results, (b) zoomed-in plot of modeling results with experimental data, (c) relative error of PC-SAFT predictions compared to experimental data.

might form synergies when acting on asphaltene precipitation and aggregation. Waxes containing large aliphatic chains interact with asphaltene and inflict steric interferences during asphaltene nucleation. This could cause the formation of more contorted asphaltene aggregates with less tendency to interact and show self-association phenomenon.

2.3. Thermodynamic Modeling. The PC-SAFT EoS was employed to predict the asphaltene phase behavior when the various wax contents were added to the system. The influence of paraffin wax on asphaltene stability zones in the crude oil at different system compositions (i.e., different gas/oil ratios) is

illustrated in Figure 8a,b. The relative errors (REs) between experimental and modeling results are also provided in Figure 8c. As can be seen, for all modified crudes with different wax contents, the model predictions are in good agreement with the experimental results. In general, the relative error was less than 6% for all experiments. However, for modified crudes with lower wax contents, more satisfactory predictions have been achieved (RE = 1.52%). A distinct deviation was observed once the model underestimated the AOP changes and did not match well with the asphaltene precipitation onset in the higher paraffin wax region (RE = 5.67%). A probable

7129

explanation for the variation between the model prediction and the QCM experimental data at high wax content may be the generalizations made in the properties of the crude oil fraction utilized as well as the uncertainties in the asphaltene structure and onset point determination in high paraffin wax-modified crude oil samples.

A comparison between the graphs for lower wax contents with those of higher wax contents in Figure 8a,b reveals that the model results present the same trend as the experimental data in shifting the asphaltene onset point and increasing the respective gas/oil ratio: AOP/GOR increases with the increase of paraffin wax content. This could be explained by the presence of heavier hydrocarbons in the crude oil and the significantly higher[56] solubility of asphaltene in hydrocarbons with a higher carbon number. In addition, this increased solubility of asphaltene widens the asphaltene stability range.

3. CONCLUSIONS

The effects of different wax inhibitors on WAT and the decrease in the pour point were evaluated first. Subsequently, the crude oil compositional modifications made as a result of the addition of several wax inhibitors and various paraffin wax content in crude oils and their influence on the asphaltene stability were investigated by monitoring changes in the asphaltene precipitation onset point and the deposition behavior of asphaltene nanoaggregates. The results indicate that it may be possible to find an optimum dosage at which the wax inhibitor can reduce both wax and asphaltene deposition problems. A wax inhibitor that is highly efficient in decreasing the viscosity might not be an appropriate chemical solution in addressing the challenge of organic deposition. Some wax inhibitors can hinder asphaltene aggregation and deposition and some of them aggravate these phenomena. The HPHT-QCM results showed that, as predicted using the thermodynamic model, wax content can decrease the asphaltene deposition rate and shift the AOP. This may be attributed to the higher solubility of asphaltenes in hydrocarbons with higher carbon number compared to those with lower carbon number. Asphaltene phase behavior in the paraffinic-modified oils was also modeled using PC-SAFT EoS. These predictions were compared with the experimental results. It was observed that the relative error was within a rational range (less than 6%) for all of the tests. However, for modified crudes with lower paraffin wax concentrations, more satisfactory predictions have been attained.

4. EXPERIMENTAL AND COMPUTATIONAL METHODS

4.1. Materials. Experiments were conducted with an additive-free crude oil from the North Sea. Table 1 presents the properties and characterization analysis of the crude oil.

Four different wax inhibitors, which were commercially sourced and denoted as INH.3, INH.4, INH.6, and INH.9, were utilized to treat the crude oil sample and investigate their effects on WAT, pour point, and asphaltene precipitation and deposition phenomena. Table 2 shows the composition and application of each inhibitor in the oilfield chemical industry.

These chemicals were chosen based on their applications and contributions in mitigating wax challenges in the industry and used as received from suppliers. For each chemical, the effective optimum concentration suggested by the suppliers (as mentioned in Table 2) has been employed in this study. A

Table 1. Characterization and Properties of Crude oil Used in This Study

properties	value
ρ_o (g mL^{-1}) at 1 atm and 20 °C	0.824
MW_o (g mol^{-1})	177
μ_o (cP) at 1 atm and 20 °C	12.2
f (g g^{-1}) (n-C$_7$ induced)	0.0355
saturates (wt %)	42.6
aromatics (wt %)	28.2
resins (wt %)	26.1
API gravity (deg)	22.4
wax content (wt %)	4.5
water content (ppm)	964

Table 2. Composition Suggested Optimum Dosage by the Supplier and Application of Each Wax Inhibitor

wax Inhibitor	chemistry	characteristics	proposed optimum dosage (ppm)
INH-3	naphthalene, 1,2,4-trimethylbenzene	wax inhibitor	400
INH-4	ethylene vinyl acetate polymer in aromatic solvent	pour point depressant	400
INH-6	mixture of surfactants and high-molecular-weight copolymers in aromatic solvent	wax and asphaltene inhibitor	350
INH-9	propriety mixture of detergents and surfactants	wax inhibitor	400

commercial paraffin wax with a melting temperature in the range of 54−56 °C, supplied by Meade-King Robinson & Co Ltd., was used in the recombination procedure, defined as the addition of a known amount of wax to the crude oil, without any additional purification. Based on the distribution of representative paraffin waxes from generic paraffinic oils, the paraffin carbon number of C$_{30}$ was chosen. Hence, the paraffin carbon number is in agreement with the reported distribution of native paraffins from typical paraffinic crude oils.[57,58] For crude oil modification with paraffin waxes or chemicals, approximately 140 g of oil and the calculated mass of each paraffin wax/chemical were heated up to 60 °C. Then, the paraffin was gently added to the crude oil sample and homogenized for at least 1 h to eschew the local concentration of the paraffin waxes or the respective chemicals. n-Heptane (n-C$_7$; >99%), anhydrous toluene (Tol; >99.8%), and ethanol (≥99.8%) were bought from Sigma-Aldrich and utilized in this study as received for washing purposes. For asphaltene deposition tests, the natural gas composition, which was injected to the QCM cell for precipitating asphaltenes, is as follows (mol %): N$_2$ (1.84%), C$_1$ (89.94%), CO$_2$ (0.91%), C$_2$ (5.32%), C$_3$ (1.45%), iso-C$_4$ (0.20%), n-C$_4$ (0.21%), iso-C$_5$ (0.07%), and (n-C$_5$) + C$_{6+}$ (0.06%).

4.2. Determination of Rheological Properties, WAT, and Wax Pour Point. The rheological properties of the studied crude oil were determined by temperature sweeps utilizing a stress-controlled rotational-type rheometer purchased from Anton Paar Ltd. (Physica MCR 301). Almost all of the measurements presented were carried out with the aid of a 25 mm diameter and 1° angle cone and plate geometry (Cones CP50-1). The setup comprises two circular plates with space in between, in which the reservoir fluid is placed. The bottom plate is fixed in rotational terms while the top is fitted to a shaft, floated on a sophisticated air bearing to keep friction

to a very low level. It is then fitted to a sensitive electric motor to control the torque of the system while rotating/oscillating according to preset experimental parameters. The gap between the lower and upper test plates is set to be 0.1 mm in length to reach the optimum measurement precision. The main reason in selecting this geometry is due to its capability to make a uniform shear rate on the thorough measuring surface area. Hence, it could generate a homogeneous flow and eliminate particle migration alongside the measuring system. Thermal equilibrium is reached easily due to the small sample volume requirement of 22 cm^3 of the setup geometry. The base plate temperature was accurately controlled within 0.1 °C in the range of −40 to +200 °C with a Peltier system. An external temperature-regulated bath (Grant, GP200) was also connected to the rheometer, set at 20 °C to cover the routine testing regime range of 30−60 °C of the measuring system. After performing primary experiments, it was illustrated that a shear rate of 10 s^{-1} would provide reproducible curves for the tested fluid. The capability of the Anton Paar, Physica MCR 301 rheometer using oscillatory mode at atmospheric conditions allows the determination of the pour point with different applied stresses. Preliminary measurements proved that a frequency of 1.59 Hz with an amplitude of 25 μN m allows data close to the pour point to be obtained from the ASTM procedure, at least for the studied oil sample. The rheometer software recorded all necessary oscillation data including deflection angle, loss modulus, and storage modulus, which were used to determine the pour point in a temperature sweep. The starting temperature and cooling rate for both WAT and pour point experiments are 50 °C and 1 °C min^{-1}, respectively. The destination temperature and shear rate for all WAT experiments are 5 °C and 10 s^{-1}, respectively. The accuracy of using the rheometer for pour point measurement was found to be ±0.2 °C, which compares well with the ASTM D97 method.[59,60]

4.3. QCM Tests. The deposition experiments were conducted at natural gas contents after reaching the asphaltene precipitation onset point. High pressure−high temperature QCM (HPHT-QCM) technique was employed to determine the onset of precipitation and monitor the comparative deposition rate. The QCM technology has been used at the Heriot-Watt Institute of Petroleum Engineering for over 20 years. Initial studies showed potential uses in some measurements relevant to the oil industry including wax, hydrates, asphaltenes, and saturation pressure and scale. Further details are given in papers by Burgass et al.[28] and Joonaki et al.[21,52,61] The principle of the measurement is to monitor changes in the resonance frequency (RF) and electrical properties at RF, for a QCM surface submersed in the test fluid, as a result of variations in the mass of the QCM or changes in the viscosity and density of the fluids brought about by changes in the temperature and/or pressure. The Sauerbrey equation[62] demonstrates how the change in the RF can be related to the alterations in mass as follows

$$\Delta f = -f_u^{3/2} \left[\frac{\rho_L \eta_L}{\Pi \rho_q \mu_q} \right]^{1/2} \tag{2}$$

where Δf and f_u are the frequency change (Hz) and the frequency of oscillation of the unloaded crystal (in air), respectively, ρ_L, η_L, ρ_q, and μ_q are the density of the liquid in contact with the electrode, the viscosity of the liquid in contact

with the electrode, the density of quartz itself, and the shear modulus of quartz for AT-cut crystal, respectively.

In this study, QCM has been used to investigate the effect of additional paraffin wax and the respective inhibitors on the AOP and deposition rate of the tested crude oil under real field-representative conditions (HPHT along with applied shear stress). The natural gas, with a composition as presented in Section 2.1, was injected at a constant rate of ∼1.1 psi/min from 600 psi. The gas at room temperature was injected into the QCM cell at 60 °C and timed to reach equilibrium. This temperature was selected to be representative of the real field condition and the condition of the paraffin waxes/chemicals, which were added to the crude oil matrix, as described in Section 2.1. The magnetic stirrer was also switched on, rotating at 500 rpm to mix the injected gas and crude oil and applied the shear stress. A schematic diagram of the QCM setup is shown in Figure 1.

4.4. PC-SAFT Equation of State. In 2001, Gross and Sadowski[63] extended the statistical associated fluid theory (SAFT), which was proposed by Chapman et al.,[64] to consider effects of chain length on the segment dispersion energy by defining dispersive interactions by extension of the perturbation theory of Barker and Henderson.[65] Of all various extensions and modification of SAFT, the PC-SAFT EoS is formulated as one of the most reliable tools to predict the phase behavior of complex fluids.[11,66,67] In particular, PC-SAFT is shown to be successful for modeling asphaltene (the heaviest and most polarizable component of crude oil) phase behavior in crude oil.[11,68,69]

In this EoS, molecules are considered as chains composed of spherical segments dividing the total intermolecular forces into reference and perturbation terms. To model bulk properties of the hydrocarbon mixtures and phase equilibria, three parameters are required for each nonassociating and nonpolar component: the segment number in the chain (m), the spherical segment diameter (σ), and the dispersion interaction energy between the segments (ε/k).

These parameters were identified by Gross and Sadowski[63] by matching the vapor pressure and the liquid volume. The authors have correlated the parameters for light gases and nonpolar hydrocarbon by fitting them to the molecular weights of the components. Moreover, for other components of live oil such as heavy gas or saturates, these parameters were taken from Gonzalez et al.,[70] which are similarly derived by fitting the parameters to the molecular weights.

For associating compounds, however, two additional parameters are required: the association energy (ε^{AB}) and the association volume (κ^{AB}). Within the PC-SAFT EoS, an improved square well potential for the segment of a chain has been used, describing the residual Helmholtz free energy. In this work, we used our in-house thermodynamic software to predict the asphaltene phase behavior, which is based on the framework of the PC-SAFT proposed by Gross and Sadowski.[63] Here, the residual Helmholtz free energy is split into two terms, the hard-chain reference fluid and the dispersion contribution

$$\tilde{a} = \tilde{a}^{hc} + \tilde{a}^{disp} \tag{3}$$

The compressibility factor is expressed through the following equation

$$Z = 1 + \eta_p \left(\frac{\partial \tilde{a}^{res}}{\partial \eta_p} \right)_{T, x_i} \tag{4}$$

The pressure (in units of Pa = N/m²) can be calculated using the following relation

$$P = Z k_B T \rho_n \left(10^{10} \frac{\text{Å}}{\text{m}} \right)^3 \tag{5}$$

According to eqs 3 and 5

$$Z = 1 + Z^{hc} + Z^{disp} \tag{6}$$

The fugacity coefficient and the chemical potentials for different components are expressed through eqs 7 and 8, respectively

$$\ln \varphi_k = \mu_k^{res}(T, v_v) / _{kT} - \ln Z \tag{7}$$

$$\mu_k^{res}(T, v_v)/_{kT} = \tilde{a}^{res} + (Z - 1) + \left(\frac{\partial \tilde{a}^{res}}{\partial x_k} \right)_{T, v, x_i \neq x_k}$$
$$- \sum_{j=1}^{N} \left[x_j \left(\frac{\partial \tilde{a}^{res}}{\partial x_j} \right)_{T, v, x_i \neq x_j} \right] \tag{8}$$

Crude oil is characterized using the SARA-based method,[68,71] considering the polydispersity of asphaltenes for an accurate prediction. Here, the same methodology as ref 68 was used for characterizing asphaltenes. Asphaltenes were divided into four pseudocomponents, namely, n-C_{8+}, n-C_{7-8}, n-C_{6-7}, and n-C_{5-6} (e.g., nC_{5-6} subfraction denotes asphaltenes insoluble in pentane, which are soluble in n-hexane, and n-C_{8+} subfraction denotes asphaltenes insoluble in n-octane). Table 3 presents

Table 3. PC-SAFT Parameters for Asphaltene Fractionation of the Crude Oil Used in This Study

component	weight percent	MW[a]	σ (Å)	m	ε/k (K)
C_{5-6} Asph, ($\gamma = 0.4$)	0.55	1837	4.24271	36.95	359.74
C_{6-7} Asph. ($\gamma = 0.4$)	0.59	2254	4.24841	45.06	360.21
C_{7-8} Asph. ($\gamma = 0.4$)	0.66	2379	4.24974	47.49	360.31
C_8 Asph. ($\gamma = 0.4$)	1.80	2640	4.25212	52.57	360.49

[a]Molecular weight of preaggregated asphaltene.

the PC-SAFT parameters of asphaltene fraction used in this work (reservoir fluid composition and the corresponding properties are provided in the Supporting Information, Tables S1 and S2). In this method, flashed gas and flashed liquid mixture, which simulates the reservoir fluid, are characterized separately. Following this, using the gas/oil ratio from the live reservoir fluid, they are mathematically merged.[72] The association term, which describes the strong short-range forces of polar components, is neglected because there were no polar molecules such as water in the system. This assumption is often secure because asphaltene phase behavior is largely set on the polarizability rather than polarity.[73]

We have employed PC-SAFT EoS within our in-house asphaltene deposition simulator,[11] where further detailed

information on the thermodynamic phase behavior modeling using PC-SAFT EoS can be found.

■ ASSOCIATED CONTENT

Ⓢℹ Supporting Information

The Supporting Information is available free of charge at https://pubs.acs.org/doi/10.1021/acsomega.9b03460.

Reservoir fluid composition; compositional groupings of the reservoir fluid (live fluid) (PDF)

■ AUTHOR INFORMATION

Corresponding Author

    Edris Joonaki − *Centre for Flow Assurance Research Studies (CFAR), Institute of GeoEnergy Engineering, School of Energy, Geoscience, Infrastructure and Society, Heriot-Watt University, Riccarton, Edinburgh EH14 4AS, U.K.; TÜV SÜD National Engineering Laboratory, East Kilbride, South Lanarkshire G75 0QF, U.K.;* ⓞ orcid.org/0000-0002-8412-0004; Email: ej5@hw.ac.uk, edris.joonaki@tuv-sud.co.uk

Authors

    Aliakbar Hassanpouryouzband − *Centre for Flow Assurance Research Studies (CFAR), Institute of GeoEnergy Engineering, School of Energy, Geoscience, Infrastructure and Society, Heriot-Watt University, Riccarton, Edinburgh EH14 4AS, U.K.; The University of Edinburgh School of GeoSciences, Grant Institute, Edinburgh EH9 3FE, U.K.;* ⓞ orcid.org/0000-0003-4183-336X

    Rod Burgass − *Centre for Flow Assurance Research Studies (CFAR), Institute of GeoEnergy Engineering, School of Energy, Geoscience, Infrastructure and Society, Heriot-Watt University, Riccarton, Edinburgh EH14 4AS, U.K.*

    Alfred Hase − *Bundrant Tech Centre, Nalco Champion, Aberdeen AB12 3HT, U.K.*

    Bahman Tohidi − *Centre for Flow Assurance Research Studies (CFAR), Institute of GeoEnergy Engineering, School of Energy, Geoscience, Infrastructure and Society, Heriot-Watt University, Riccarton, Edinburgh EH14 4AS, U.K.*

Complete contact information is available at:
https://pubs.acs.org/10.1021/acsomega.9b03460

Notes

The authors declare no competing financial interest.

■ ACKNOWLEDGMENTS

■ REFERENCES

(1) Mehrabian, H.; Bellucci, M. A.; Walsh, M. R.; Trout, B. L. Effect of Salt on Antiagglomerant Surface Adsorption in Natural Gas Hydrates. *J. Phys. Chem. C* **2018**, *122*, 12839−12849.

(2) Redelius, P. Bitumen Solubility Model Using Hansen Solubility Parameter. *Energy Fuels* **2004**, *18*, 1087−1092.

(3) Musser, B. J.; Kilpatrick, P. K. Molecular Characterization of Wax Isolated from a Variety of Crude Oils. *Energy Fuels* **1998**, *12*, 715−725.

(4) García, M. C. Crude Oil Wax Crystallization. The Effect of Heavy *n*-Paraffins and Flocculated Asphaltenes. *Energy Fuels* **2000**, *14*, 1043−1048.

(5) Carbognani, L.; DeLima, L.; Orea, M.; Ehrmann, U. Studies on Large Crude Oil Alkanes. II. Isolation and Characterization of Aromatic Waxes and Waxy Asphaltenes. *Pet. Sci. Technol.* **2000**, *18*, 607−634.

(6) Joonaki, E.; Youzband, A. H.; Burgass, R.; Tohidi, B. In *Effect of Water Chemistry on Asphaltene Stabilised Water in Oil Emulsions-A New Search for Low Salinity Water Injection Mechanism*, 79th EAGE Conference and Exhibition; European Association of Geoscientists & Engineers, 2017.

(7) Nassar, N. N. Asphaltene Adsorption onto Alumina Nanoparticles: Kinetics and Thermodynamic Studies. *Energy Fuels* **2010**, *24*, 4116−4122.

(8) Dechaine, G. P.; Gray, M. R. Chemistry and Association of Vanadium Compounds in Heavy Oil and Bitumen, and Implications for Their Selective Removal. *Energy Fuels* **2010**, *24*, 2795−2808.

(9) Andersen, S. I.; Jensen, J. O.; Speight, J. G. X-Ray Diffraction of Subfractions of Petroleum Asphaltenes. *Energy Fuels* **2005**, *19*, 2371−2377.

(10) Adams, J. J. Asphaltene Adsorption, a Literature Review. *Energy Fuels* **2014**, *28*, 2831−2856.

(11) Hassanpouryouzband, A.; Joonaki, E.; Taghikhani, V.; Bozorgmehry Boozarjomehry, R.; Chapoy, A.; Tohidi, B. New Two-Dimensional Particle-Scale Model To Simulate Asphaltene Deposition in Wellbores and Pipelines. *Energy Fuels* **2017**, *32*, 2661−2672.

(12) Wang, S.; Liu, J.; Zhang, L.; Xu, Z.; Masliyah, J. Colloidal Interactions between Asphaltene Surfaces in Toluene. *Energy Fuels* **2009**, *23*, 862−869.

(13) Movahedi, H.; Farahani, M. V.; Jamshidi, S. Application of Hydrated Basil Seeds (HBS) as the Herbal Fiber on Hole Cleaning and Filtration Control. *J. Pet. Sci. Eng.* **2017**, *152*, 212−228.

(14) Monjezi, E.; Rostami, A.; Joonaki, E.; Shadizadeh, S. R. New Application of Henna Extract as an Asphaltene Inhibitor: An Experimental Study. *Asia-Pac. J. Chem. Eng.* **2016**, *11*, 1027−1034.

(15) Taheri-Shakib, J.; Hosseini, S. A.; Kazemzadeh, E.; Keshavarz, V.; Rajabi-Kochi, M.; Naderi, H. Experimental and Mathematical Model Evaluation of Asphaltene Fractionation Based on Adsorption in Porous Media: Dolomite Reservoir Rock. *Fuel* **2019**, *245*, 570−585.

(16) Taheri-Shakib, J.; Keshavarz, V.; Kazemzadeh, E.; Hosseini, S. A.; Rajabi-Kochi, M.; Salimidelshad, Y.; Naderi, H.; Bakhtiari, H. A. Experimental and Mathematical Model Evaluation of Asphaltene Fractionation Based on Adsorption in Porous Media: Part 1. Calcite Reservoir Rock. *J. Pet. Sci. Eng.* **2019**, *177*, 24−40.

(17) Al-Jabri, J.; Sultan, A.; Al-Mutairi, E.; Onaizi, S. A.; Merghani, A.; Hassen, I. In *Screening New Formulations for Asphaltene Aggregation Inhibition*, SPE Kingdom of Saudi Arabia Annual Technical Symposium and Exhibition; Society of Petroleum Engineers,2018.

(18) Speight, J. G. *The Chemistry and Technology of Petroleum*; CRC Press, 2014.

(19) Wiehe, I. A. *Process Chemistry of Petroleum Macromolecules*; CRC Press, 2008.

(20) Chaisoontornyotin, W.; Haji-Akbari, N.; Fogler, H. S.; Hoepfner, M. P. Combined Asphaltene Aggregation and Deposition Investigation. *Energy Fuels* **2016**, *30*, 1979−1986.

(21) Joonaki, E.; Buckman, J.; Burgass, R.; Tohidi, B. Water versus Asphaltenes; Liquid−Liquid and Solid−Liquid Molecular Interactions Unravel the Mechanisms behind an Improved Oil Recovery Methodology. *Sci. Rep.* **2019**, *9*, No. 11369.

(22) Kelland, M. A. *Production Chemicals for the Oil and Gas Industry*; CRC Press, 2010; Vol. 72.

(23) Subramanian, S.; Simon, S.; Gao, B.; Sjöblom, J. Asphaltene Fractionation Based on Adsorption onto Calcium Carbonate: Part 1: Characterization of Sub-Fractions and QCM-Measurements. *Colloids Surf., A* **2016**, *495*, 136−148.

(24) Ameri Mahabadian, M.; Chapoy, A.; Tohidi, B. A New Thermodynamic Model for Paraffin Precipitation in Highly Asymmetric Systems at High Pressure Conditions. *Ind. Eng. Chem. Res.* **2016**, *55*, 10208−10217.

(25) Paso, K.; Kallevik, H.; Sjoblom, J. Measurement of Wax Appearance Temperature Using Near-Infrared (NIR) Scattering. *Energy Fuels* **2009**, *23*, 4988−4994.

(26) Marchesini, F. H.; Alicke, A. A.; de Souza Mendes, P. R.; Ziglio, C. M. Rheological Characterization of Waxy Crude Oils: Sample Preparation. *Energy Fuels* **2012**, *26*, 2566−2577.

(27) Espada, J. J.; Coutinho, J. A. P.; Pena, J. L. Evaluation of Methods for the Extraction and Characterization of Waxes from Crude Oils. *Energy Fuels* **2010**, *24*, 1837−1843.

(28) Burgass, R. W.; Tohidi, B. Development and Validation of Small Volume Multi-Tasking Flow Assurance Tool. In *SPE Asia Pacific Oil and Gas Conference and Exhibition*; 2011; Vol. M. https://doi.org/10.2118/145946-MS.

(29) ASTM.Standard Test Method for Pour Point of Petroleum Products, In *Annual Book of ASTM Standards*; ASTM, 1996.

(30) Machado, A. L. C.; Lucas, E. F. Influence of Ethylene-co-vinyl Acetate Copolymers on the Flow Properties of Wax Synthetic Systems. *J. Appl. Polym. Sci.* **2002**, *85*, 1337−1348.

(31) Wei, B. Recent Advances on Mitigating Wax Problem Using Polymeric Wax Crystal Modifier. *J. Pet. Explor. Prod. Technol.* **2015**, *5*, 391−401.

(32) Yang, X.; Kilpatrick, P. Asphaltenes and Waxes Do Not Interact Synergistically and Coprecipitate in Solid Organic Deposits. *Energy Fuels* **2005**, *19*, 1360−1375.

(33) Venkatesan, R.; Östlund, J.-A.; Chawla, H.; Wattana, P.; Nydén, M.; Fogler, H. S. The Effect of Asphaltenes on the Gelation of Waxy Oils. *Energy Fuels* **2003**, *17*, 1630−1640.

(34) García, M. C.; Carbognani, L. Asphaltene− Paraffin Structural Interactions. Effect on Crude Oil Stability. *Energy Fuels* **2001**, *15*, 1021−1027.

(35) Maqbool, T.; Balgoa, A. T.; Fogler, H. S. Revisiting Asphaltene Precipitation from Crude Oils: A Case of Neglected Kinetic Effects. *Energy Fuels* **2009**, *23*, 3681−3686.

(36) Kraiwattanawong, K.; Fogler, H. S.; Gharfeh, S. G.; Singh, P.; Thomason, W. H.; Chavadej, S. Effect of Asphaltene Dispersants on Aggregate Size Distribution and Growth. *Energy Fuels* **2009**, *23*, 1575−1582.

(37) Castillo, J.; Gutierrez, H.; Ranaudo, M.; Villarroel, O. Measurement of the Refractive Index of Crude Oil and Asphaltene Solutions: Onset Flocculation Determination. *Energy Fuels* **2010**, *24*, 492−495.

(38) Yang, Z.; Chen, S.; Peng, H.; Li, M.; Lin, M.; Dong, Z.; Zhang, J.; Ji, Y. Effect of Precipitating Environment on Asphaltene Precipitation: Precipitant, Concentration, and Temperature. *Colloids Surf., A* **2016**, *497*, 327−335.

(39) Powers, D. P.; Sadeghi, H.; Yarranton, H. W.; Van Den Berg, F. G. A. Regular Solution Based Approach to Modeling Asphaltene Precipitation from Native and Reacted Oils: Part 1, Molecular Weight, Density, and Solubility Parameter Distributions of Asphaltenes. *Fuel* **2016**, *178*, 218−233.

(40) Barrera, D. M.; Ortiz, D. P.; Yarranton, H. W. Molecular Weight and Density Distributions of Asphaltenes from Crude Oils. *Energy Fuels* **2013**, *27*, 2474−2487.

(41) Tharanivasan, A. K.; Yarranton, H. W.; Taylor, S. D. Application of a Regular Solution-Based Model to Asphaltene Precipitation from Live Oils. *Energy Fuels* **2011**, *25*, 528−538.

(42) Díaz, O. C.; Modaresghazani, J.; Satyro, M. A.; Yarranton, H. W. Modeling the Phase Behavior of Heavy Oil and Solvent Mixtures. *Fluid Phase Equilib.* **2011**, *304*, 74−85.

(43) Haji-Akbari, N.; Teeraphapkul, P.; Balgoa, A. T.; Fogler, H. S. Effect of N-Alkane Precipitants on Aggregation Kinetics of Asphaltenes. *Energy Fuels* **2015**, *29*, 2190−2196.

(44) Wiehe, I. A.; Yarranton, H. W.; Akbarzadeh, K.; Rahimi, P. M.; Teclemariam, A. The Paradox of Asphaltene Precipitation with Normal Paraffins. *Energy Fuels* **2005**, *19*, 1261−1267.

(45) Yanes, J. F. R.; Feitosa, F. X.; do Carmo, F. R.; de Sant'Ana, H. B. Paraffin Effects on the Stability and Precipitation of Crude Oil Asphaltenes: Experimental Onset Determination and Phase Behavior Approach. *Fluid Phase Equilib.* **2018**, *474*, 116−125.

(46) Wang, J. X.; Buckley, J. S. A Two-Component Solubility Model of the Onset of Asphaltene Flocculation in Crude Oils. *Energy Fuels* **2001**, *15*, 1004–1012.

(47) Zuo, J. Y.; Mullins, O. C.; Freed, D.; Elshahawi, H.; Dong, C.; Seifert, D. J. Advances in the Flory–Huggins–Zuo Equation of State for Asphaltene Gradients and Formation Evaluation. *Energy Fuels* **2013**, *27*, 1722–1735.

(48) Freed, D. E.; Mullins, O. C.; Zuo, J. Y. Theoretical Treatment of Asphaltene Gradients in the Presence of GOR Gradients. *Energy Fuels* **2010**, *24*, 3942–3949.

(49) Alboudwarej, H.; Akbarzadeh, K.; Beck, J.; Svrcek, W. Y.; Yarranton, H. W. Regular Solution Model for Asphaltene Precipitation from Bitumens and Solvents. *AIChE J.* **2003**, *49*, 2948–2956.

(50) Wang, J. Predicting Asphaltene Flocculation in Crude Oils, In. *New Mexico Institute of Mining and Technology*; Petroleum Engineering, 2000.

(51) Roenningsen, H. P.; Bjoerndal, B.; Baltzer Hansen, A.; Batsberg Pedersen, W. Wax Precipitation from North Sea Crude Oils: 1. Crystallization and Dissolution Temperatures, and Newtonian and Non-Newtonian Flow Properties. *Energy Fuels* **1991**, *5*, 895–908.

(52) Joonaki, E.; Buckman, J.; Burgass, R.; Tohidi, B. Exploration of the Difference in Molecular Structure of N-C7 and CO2 Induced Asphaltenes. *Ind. Eng. Chem. Res.* **2018**, *57*, 8810–8818.

(53) Buenrostro-Gonzalez, E.; Groenzin, H.; Lira-Galeana, C.; Mullins, O. C. The Overriding Chemical Principles That Define Asphaltenes. *Energy Fuels* **2001**, *15*, 972–978.

(54) McKenna, A. M.; Marshall, A. G.; Rodgers, R. P. Heavy Petroleum Composition. 4. Asphaltene Compositional Space. *Energy Fuels* **2013**, *27*, 1257–1267.

(55) Sedghi, M.; Goual, L.; Welch, W.; Kubelka, J. Effect of Asphaltene Structure on Association and Aggregation Using Molecular Dynamics. *J. Phys. Chem. B* **2013**, *117*, 5765–5776.

(56) Andersen, S. I.; Speight, J. G. Thermodynamic Models for Asphaltene Solubility and Precipitation. *J. Pet. Sci. Eng.* **1999**, *22*, 53–66.

(57) Ganeeva, Y. M.; Yusupova, T. N.; Romanov, G. V. Waxes in Asphaltenes of Crude Oils and Wax Deposits. *Pet. Sci.* **2016**, *13*, 737–745.

(58) Ganeeva, Y. M.; Foss, T. R.; Yusupova, T. N.; Romanov, A. G. Distribution of High-Molecular-Weight n-Alkanes in Paraffinic Crude Oils and Asphaltene-Resin-Paraffin Deposits. *Pet. Chem.* **2010**, *50*, 17–22.

(59) Visintin, R. F. G.; Lapasin, R.; Vignati, E.; D'Antona, P.; Lockhart, T. P. Rheological Behavior and Structural Interpretation of Waxy Crude Oil Gels. *Langmuir* **2005**, *21*, 6240–6249.

(60) Kané, M.; Djabourov, M.; Volle, J.-L. Rheology and Structure of Waxy Crude Oils in Quiescent and under Shearing Conditions. *Fuel* **2004**, *83*, 1591–1605.

(61) Joonaki, E.; Burgass, R.; Hassanpouryouzband, A.; Tohidi, B. Comparison of Experimental Techniques for Evaluation of Chemistries against Asphaltene Aggregation and Deposition: New Application of High-Pressure and High-Temperature Quartz Crystal Microbalance. *Energy Fuels* **2017**, *32*, 2712–2721.

(62) Sauerbrey, G. Verwendung von Schwingquarzen Zur Wägung Dünner Schichten Und Zur Mikrowägung. *Z. Phys.* **1959**, *155*, 206–222.

(63) Gross, J.; Sadowski, G. Perturbed-Chain SAFT: An Equation of State Based on a Perturbation Theory for Chain Molecules. *Ind. Eng. Chem. Res.* **2001**, *40*, 1244–1260.

(64) Chapman, W. G.; Gubbins, K. E.; Jackson, G.; Radosz, M. New Reference Equation of State for Associating Liquids. *Ind. Eng. Chem. Res.* **1990**, *29*, 1709–1721.

(65) Barker, J. A.; Henderson, D. Perturbation Theory and Equation of State for Fluids. II. A Successful Theory of Liquids. *J. Chem. Phys.* **1967**, *47*, 4714–4721.

(66) Hassanpouryouzband, A.; Farahani, M. V.; Yang, J.; Tohidi, B.; Chuvilin, E.; Istomin, V.; Bukhanov, B. Solubility of Flue Gas or Carbon Dioxide-Nitrogen Gas Mixtures in Water and Aqueous Solutions of Salts: Experimental Measurement and Thermodynamic Modeling. *Ind. Eng. Chem. Res.* **2019**, *58*, 3377–3394.

(67) Hasanvand, M. Z.; Montazeri, M.; Salehzadeh, M.; Amiri, M.; Fathinasab, M. A Literature Review of Asphaltene Entity, Precipitation, and Deposition: Introducing Recent Models of Deposition in the Well Column. *J. Oil, Gas Petrochem. Sci.* **2018**, *1*, 83–89.

(68) Tavakkoli, M.; Chen, A.; Vargas, F. M. Rethinking the Modeling Approach for Asphaltene Precipitation Using the PC-SAFT Equation of State. *Fluid Phase Equilib.* **2016**, *416*, 120–129.

(69) Panuganti, S. R.; Tavakkoli, M.; Vargas, F. M.; Gonzalez, D. L.; Chapman, W. G. SAFT Model for Upstream Asphaltene Applications. *Fluid Phase Equilib.* **2013**, *359*, 2–16.

(70) Gonzalez, D. L.; Hirasaki, G. J.; Creek, J.; Chapman, W. G. Modeling of Asphaltene Precipitation Due to Changes in Composition Using the Perturbed Chain Statistical Associating Fluid Theory Equation of State. *Energy Fuels* **2007**, *21*, 1231–1242.

(71) Panuganti, S. R.; Vargas, F. M.; Gonzalez, D. L.; Kurup, A. S.; Chapman, W. G. PC-SAFT Characterization of Crude Oils and Modeling of Asphaltene Phase Behavior. *Fuel* **2012**, *93*, 658–669.

(72) Sisco, C.; Abutaqiya, M. I. L.; Wang, F.; Zhang, J.; Tavakkoli, M.; Vargas, F. M. Asphaltene Precipitation Modeling, In *Asphaltene Deposition*; CRC Press, 2018; pp 111–159.

(73) Buckley, J. S. Predicting the Onset of Asphaltene Precipitation from Refractive Index Measurements. *Energy Fuels* **1999**, *13*, 328–332.